Available online at www.scholarsresearchlibrary.com

Scholars Research Library

Der Pharmacia Lettre, 2016, 8 (4):289-298
(http://scholarsresearchlibrary.com/archive.html)

ISSN 0975-5071
USA CODEN: DPLEB4

Experimental and computational studies for new quinoline derivative as inhibitor for carbon steel in hydrochloric acid

Y. Bouzian[1], A. Elyoussfi[2], A. Dafali[2], R. Bouhfid[3], H. Elmsellem[2], M. M. Abdelahi[1], A. Nadeem[1], A. Zarrouk[2], A. L. Essaghouani[1] and E. M. Essassi[1]

[1]Laboratoire de Chimie Organique Hétérocyclique, URAC 21, Pôle de Compétences Pharmacochimie, Université Mohammed V, Faculté des Sciences, Av. Ibn Battouta, BP 1014 Rabat, Morocco
[2]LCAE-URAC 18, Faculty of Science, First Mohammed University, PO Box 717, 60 000 Oujda, Morocco
[3]Moroccan Foundation for Advanced Science, Innovation and Research (MASCIR), Institut of Nanomaterials and Nanotechnology, Rabat, Morocco

---

ABSTRACT

The inhibiting action of 2-oxo-1,2-dihydroquinoline-4-carboxylic acid (Q1) on the corrosion of carbon steel in hydrochloric acid has been studied using weight loss, potentiodynamic polarization and electrochemical impedance spectroscopy (EIS) techniques. The inhibition efficiency increases with increase in inhibitor concentration. Impedance measurements showed that the double-layer capacitance decreased and charge-transfer resistance increased with increase in the inhibitor concentration and hence increasing in inhibition efficiency. Polarization curves show that Q1 is a mixed-type inhibitor. The adsorption of Q1 onto the carbon steel surface was found to follow the Langmuir adsorption isotherm. Quantum chemical parameters such as highest occupied molecular orbital energy (E_{HOMO}), lowest unoccupied molecular orbital energy (E_{LUMO}), energy gap (ΔE) and dipole moment (μ) were calculated. Quantum chemical calculations also supported experimental data and the adsorption of inhibitor molecules onto the metal surface.

Keywords*:* Carbon steel, HCl, Corrosion inhibition, Weight loss, Electrochemical studies, DFT.

INTRODUCTION

The corrosion of materials is one of the main problems facing industrial processes, generating huge financial losses. Metallic industrial structures are often exposed to conditions that facilitate corrosive processes. For example, acidic solutions, which are widely used in acid pickling, industrial acid cleaning and oil refinery equipment cleaning, promote the acceleration of metallic corrosion, affecting the performance and durability of the treated equipment [1,2].

The use of organic inhibitors for preventing corrosion is a promising alternative solution. These inhibitors are usually adsorbed on the metal surface by the formation of a coordinate covalent bond (chemical adsorption) or the electrostatic interaction between the metal and inhibitor (physical adsorption) [3]. This adsorption produces a uniform film on the metal surface, which reduces or prevents contact with the corrosive medium [4].

Most of the effective organic inhibitors used contain heteroatoms such as O, N, S and multiple bonds in their molecules through which they are adsorbed on the metal surface [5-31]. It has been observed that adsorption depends mainly on certain physico-chemical properties of the inhibitor group, such as functional groups, electron density at the donor atom, π-orbital character, and the electronic structure of the molecule [32]. One technique that has been used to evaluate organic corrosion inhibitors is molecular modeling. Through quantum chemical calculations, it is possible to obtain structural parameters, such as the energies of the frontier molecular orbitals, the

HOMO (highest occupied molecular orbital) and LUMO (lowest unoccupied molecular orbital), and the dipole moment. These parameters influence the potential inhibition and are generally strongly correlated with the experimentally obtained inhibition efficiency [33-36]. Thus, this technique is an important tool for pre-selecting possible corrosion inhibitors and studying the correlation between molecular structure and corrosion inhibition efficiency [37].

The present work was established to study the corrosion inhibition of carbon steel in 1 M HCl solution by new quinoline derivatives as corrosion inhibitor using different techniques: weight loss, potentiodynamic polarization and electrochemical impedance spectroscopy (EIS). Quantum chemical study using density functional theory (DFT) was further employed in an attempt to correlate the inhibitive effect with the molecular structure of 2-oxo-1,2-dihydroquinoline-4-carboxylic acid (Q1).

MATERIALS AND METHODS

Materials

The steel used in this study is a carbon steel (CS) (Euronorm: C35E carbon steel and US specification: SAE 1035) with a chemical composition (in wt%) of 0.370 % C, 0.230 % Si, 0.680 % Mn, 0.016 % S, 0.077 % Cr, 0.011 % Ti, 0.059 % Ni, 0.009 % Co, 0.160 % Cu and the remainder iron (Fe).

Synthesis

To a solution of isatin (10 mmole) and malonic acid (10 mmole) in acetic acid 30 ml, was added sodium acetate (1 mmole). The mixture was refluxed for 24 hours. After cooling ice-water (100ml) was added. The obtained precipate washed several time with ethanol, to lead compound Q1.

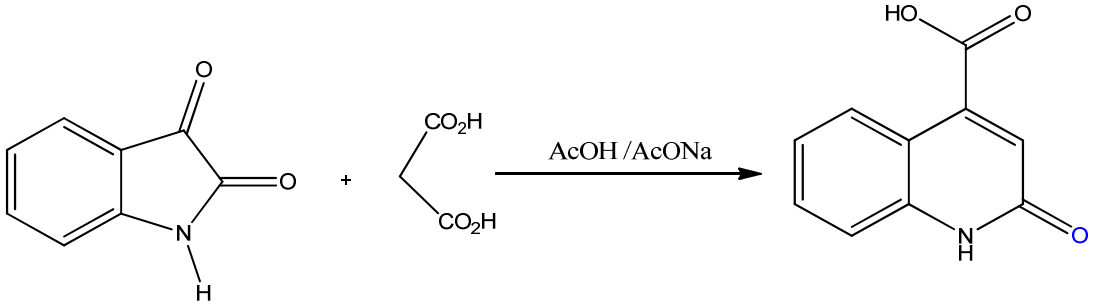

Rdt = 87 %.F > 250 °C (EtOH). Spectre de RMN 1H (DMSOd6): 7.14(s, 1H, CH); 7.68-8.63(m, 4H, CHAr). Spectre de RMN 13C (DMSOd6) : 120.6 (=CH); 117.1, 117.6, 126.7, 133.7 (CHAr); 118.3, 137.0, 142.7 (Cq); 163.5 (C=O); 169.5 (CO2H). Spectre IR (cm-1) 3210 νN−H ; 2900-3100 νO-H ; 1705 νC=O. Spectre de masse (IE) M (m/z) = 189.

Solutions

The aggressive solutions of 1 M HCl were prepared by dilution of analytical grade 37% HCl with distilled water. The concentration range of 2-oxo-1,2-dihydroquinoline-4-carboxylic acid (Q1) used was 10^{-6} M to 10^{-3} M.

Gravimetric study

Gravimetric experiments were performed according to the standard methods [38], the carbon steel sheets of 1 × 1 × 0.1 cm were abraded with a series of emery papers SiC (120, 600 and 1200) and then washed with distilled water and acetone. After weighing accurately, the specimens were immersed in a 100 mL beaker containing 250 mL of 1 M HCl solution with and without addition of different concentrations inhibitor. All the aggressive acid solutions were open to air. After 6 h of acid immersion, the specimens were taken out, washed, dried, and weighed accurately. In order to get good reproducibility, all measurements were performed few times and average values were reported to obtain good reproducibility. The inhibition efficiency (η_{WL}%) and surface coverage (θ) were calculated as follows:

$$C_R = \frac{W_b - W_a}{At} \quad (1)$$

$$\eta_{WL}(\%) = \left(1 - \frac{w_i}{w_0}\right) \times 100 \quad (2)$$

$$\theta = \left(1 - \frac{w_i}{w_0}\right) \quad (3)$$

where W_b and W_a are the specimen weight before and after immersion in the tested solution, w_0 and w_i are the values of corrosion weight losses of carbon steel in uninhibited and inhibited solutions, respectively, A the total area of the carbon steel specimen (cm^2) and t is the exposure time (h).

Electrochemical measurements

Electrochemical impedance spectroscopy

The electrochemical measurements were carried out using Volta lab (Tacussel- Radiometer PGZ 100) potentiostate and controlled by Tacussel corrosion analysis software model (Voltamaster 4) at under static condition. The corrosion cell used had three electrodes. The reference electrode was a saturated calomel electrode (SCE). A platinum electrode was used as auxiliary electrode of surface area of 1 cm^2. The working electrode was carbon steel. All potentials given in this study were referred to this reference electrode. The working electrode was immersed in test solution for 30 minutes to a establish steady state open circuit potential (E_{ocp}). After measuring the E_{ocp}, the electrochemical measurements were performed. All electrochemical tests have been performed in aerated solutions at 308 K. The EIS experiments were conducted in the frequency range with high limit of 100 kHz and different low limit

0.1 Hz at open circuit potential, with 10 points per decade, at the rest potential, after 30 min of acid immersion, by applying 10 mV ac voltage peak-to-peak. Nyquist plots were made from these experiments. The best semicircle can be fit through the data points in the Nyquist plot using a non-linear least square fit so as to give the intersections with the *x*-axis.

The inhibition efficiency of the inhibitor was calculated from the charge transfer resistance values using the following equation:

$$\eta_z\% = \frac{R_{ct}^i - R_{ct}^\circ}{R_{ct}^i} \times 100 \quad (4)$$

where, R_{ct}° and R_{ct}^i are the charge transfer resistance in absence and in presence of inhibitor, respectively.

Potentiodynamic polarization

The electrochemical behaviour of carbon steel sample in inhibited and uninhibited solution was studied by recording anodic and cathodic potentiodynamic polarization curves. Measurements were performed in the 1 M HCl solution containing different concentrations of the tested inhibitor by changing the electrode potential automatically from -600 to -300 mV versus corrosion potential at a scan rate of 1 mV s^{-1}. The linear Tafel segments of anodic and cathodic curves were extrapolated to corrosion potential to obtain corrosion current densities (I_{corr}). From the polarization curves obtained, the corrosion current (I_{corr}) was calculated by extrapolation of the linear segments of cathodic and anodic Tafel curves.

The inhibition efficiency was evaluated from the measured I_{corr} values using the relationship:

$$\eta_{Tafel}\% = \frac{I_{corr}^\circ - I_{corr}^i}{I_{corr}^\circ} \times 100 \quad (5)$$

where, I_{corr}° and I_{corr}^i are the corrosion current density in absence and presence of inhibitor, respectively.

Quantum chemical calculations

Complete geometrical optimizations of the investigated molecules are performed using DFT (density functional theory) with the Beck's three parameter exchange functional along with the Lee-Yang-Parr nonlocal correlation functional (B3LYP) [39-41] with 6-31G* basis set is implemented in Gaussian 03 program package [42]. This approach is shown to yield favorable geometries for a wide variety of systems. This basis set gives good geometry optimizations. The geometry structure was optimized under no constraint. The following quantum chemical parameters were calculated from the obtained optimized structure: The highest occupied molecular orbital (E_{HOMO})

and the lowest unoccupied molecular orbital (E_{LUMO}), the energy difference (ΔE) between E_{HOMO} and E_{LUMO} and dipole moment (μ).

RESULTS AND DISCUSSION

Potentiodynamic polarization study

The potentiodynamic polarization measurements were undertaken in order to study the effect of investigated inhibitor (Q1) on the anodic carbon steel dissolution and cathodic hydrogen evolution reactions. The polarization curves for carbon steel dissolution in the absence and presence of different concentrations of the studied inhibitor are shown in Fig. 1. Extrapolation of the linear segments of cathodic and anodic Tafel curves furnished essential corrosion parameters such as corrosion potential (E_{corr}), corrosion current density (I_{corr}) and cathodic Tafel slopes (β_c). These polarization parameters along with calculated inhibition efficiency (η_{Tafel}%) are presented in Table 1.

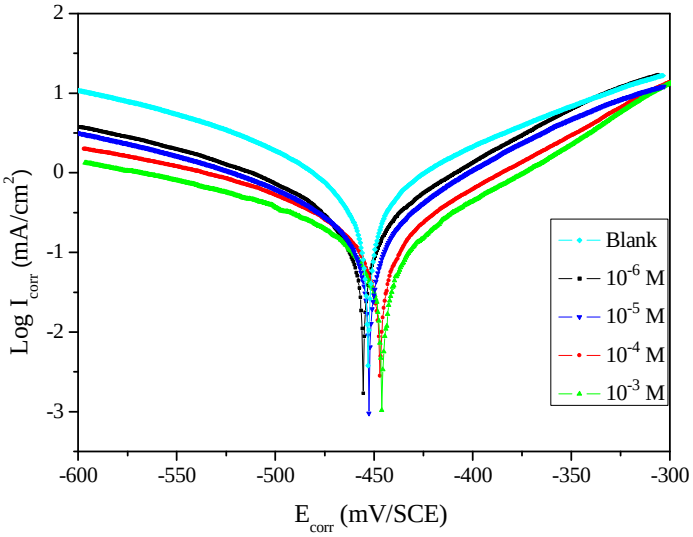

Figure 1: Potentiodynamic polarization curves for carbon steel in 1 M HCl containing different concentrations of Q1

It can be seen from Fig. 1 that the addition of Q1 causes a remarkable decrease in the current densities, indicating that both anodic metal dissolution and cathodic hydrogen evolution reactions are drastically suppressed. Meanwhile, this suppression effect of the process is more pronounced with the increasing concentration of Q1. Moreover, the cathodic Tafel curves give rise to almost parallel lines, which means that addition of Q1 doesn't modify the hydrogen evolution mechanism and the adsorbed Q1 molecules on the carbon steel surface only block the active sites of hydrogen evolution. On the other hand, it is apparent that the anodic reaction is evidently inhibited in the presence of Q1 and the shape of anodic Tafel curves in the inhibited solution slightly changes with contrast to that in the blank solution.

Table 1: Potentiodynamic polarizations parameters of carbon steel in 1 M HCl for various concentrations of Q1

Medium	Conc (M)	$-E_{corr}$ (mV_{SCE})	$-\beta_c$ (mV/dec)	I_{corr} ($\mu A\ cm^{-2}$)	η_{Tafel} (%)
Blank	1.0	453	143.0	1559.0	—
Q1	10^{-3}	446	145.3	150.0	90
	10^{-4}	455	153.3	203.5	87
	10^{-5}	445	178.2	316.0	80
	10^{-6}	452	161.9	457.0	71

From the results shown in Table, it is observed that the presence of Q1 in acid solution affects the anodic rate of carbon steel dissolution as well as rate of cathodic hydrogen evolution without causing any substantial decrease in the value of E_{corr} suggesting that Q1 is a mixed type inhibitor [43,44]. Further, results showed that the presence of Q1 decreases the values of corrosion current density (I_{corr}) suggesting that rate of carbon steel dissolution decreased in the presence of Q1 at various concentrations [45]. Further, decrease in I_{corr} values is more pronounced at higher Q1 concentration.

Electrochemical impedance spectroscopy

In order to study the effectiveness of the present inhibitor, EIS was recorded for carbon steel in the presence and absence of inhibitor with constant time. The effect of the inhibitor concentration on the impedance behavior of carbon steel in 1 M HCl solution is presented in Fig. 2. The impedance spectra show that as the inhibitor concentration increases, the diameter of the semicircle increases. The results clearly indicate that quinoline derivative inhibits the corrosion of carbon steel in 1 M HCl at any concentration used, and the inhibition efficiency (η) increases continuously with increasing concentration. The maximum η (%) is observed to be 91 at 10^{-3} M for 1 M HCl, as shown in Table 2.

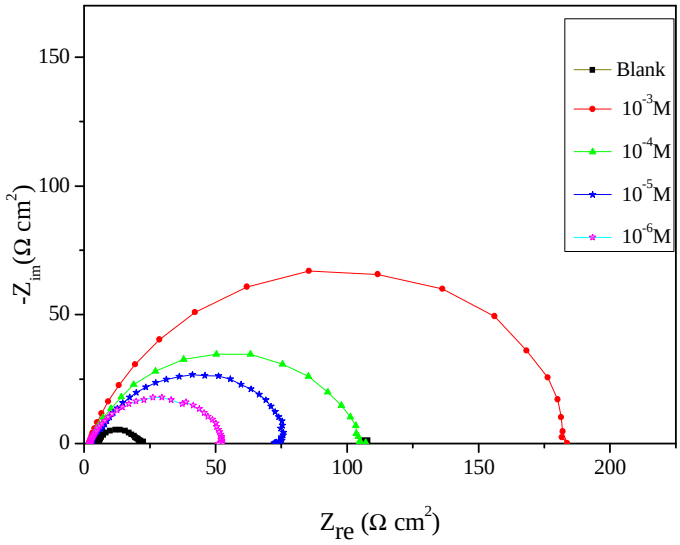

Figure 2: Electrochemical impedance response of carbon steel in 1 M HCl solution in the presence of different concentrations of Q1

Table 2: Electrochemical impedance parameters of carbon steel in 1 M HCl solution in the absence and in the presence of various concentrations of the inhibitor at 308 K

Medium	Conc (M)	R_{ct} (Ω cm^2)	C_{dl} (μF cm^{-2})	f_{max} (Hz)	η_Z (%)
Blank	1.0	16.6	200	48.0	—
Q1	10^{-3}	183	54.9	15.8	91
	10^{-4}	103	61.5	25.1	84
	10^{-5}	71.0	70.8	31.6	77
	10^{-6}	50.5	78.7	40.0	67

Data in Table 2 reveal that R_{ct} value increase with increasing inhibitor concentration and C_{dl} values decrease in the presence of the inhibitor. This is due to the adsorption of inhibitor molecules on the metal/solution interface. A decrease in local dielectric constant and/or an increase in the thickness of the electrical double layer can cause decrease in C_{dl} values, which suggests the replacement of adsorbed water molecules with high dielectric constant by inhibitor molecules with low dielectric constant. According to Helmholtz model, this phenomen on can be discussed in which the double layer capacitanceis inversely proportional to the surface changes as shown in the following equation [46]:

$$C_{dl} = \frac{\varepsilon_0 \varepsilon A}{d} \qquad (6)$$

where, ε_o: the permittivity of air (8.854×10^{-14}F/cm), ε: the local dielectric constant of the medium, d: the thickness of the film and A: the surface area of the electrode. The impedance results showed smaller C_{dl} values for the inhibited solution compared to those obtained in case of uninhibited solution (without inhibitor). The decrease in C_{dl} values is resulted from the decrease in the local dielectric constant and/or an increase in the thickness of the electrical double layer. This describes the role of inhibitor molecules, and shows that their function is performed by adsorption on the metal/solution interface [47]. Inhibition efficiencies obtained from potentiodynamic polarization curves and EIS are in good reasonably agreement which indicates the reproducility of the two methods.

Weight loss measurements

The corrosion parameters like corrosion rate (C_R), surface coverage (θ) and inhibition efficiency(η_{WL}%) of the corrosion inhibitor (Q1) in the concentration range of 10^{-6} to 10^{-3} M at 308 K are shown in Table 3. It is clear that the corrosion rate decreases and inhibition efficiency (η_{WL}%) increases with increasing concentration of the inhibitor and reaches maximum at the concentration of 10^{-3} M. It may be due to blocking of the active sites on the carbon steel surface with the inhibitor molecules that reduces the attack of corrosive solution on the carbon steel surface.

Table 3: Gravimetric results of steel corrosion in 1 M HCl (6 h immersion) without and with various concentrations of Q1 at 308 K

Medium	Conc (M)	C_R (mg cm^{-2} h^{-1})	η_{WL} (%)	θ
Blank	1.0	0.910	—	—
Q1	10^{-3}	0.082	91.0	0.910
	10^{-4}	0.127	86.0	0.860
	10^{-5}	0.173	81.2	0.812
	10^{-6}	0.235	74.2	0.742

Adsorption isotherm

Adsorption strength can be deduced from the adsorption isotherm, which shows the equilibrium relation ship between concentrations of inhibitors on the surface and in the bulk of the solution [48-50]. Important information about the interaction of the synthesized quinoline derivative and metal surface were given using adsorption isotherm. Two main types of interaction (mechanism) can describe the adsorption behaviour of the inhibitors: physisorption and chemisorption [51]. The type of interaction depends on: the chemical structure of the inhibitors, the temperature during the experiments, the electrochemical potential, the charge, and nature of the metal. The adsorption of organic inhibitor molecules on the metal surface can be considered as a quasisubstitution process between the organic compounds in the aqueous phase [$Org_{(sol)}$] and water molecules associated with the metallic surface [$H_2O_{(ads)}$] as represented by the following equilibrium [50,51]:

$$Org_{(sol)} + xH_2O_{(ads)} \leftrightarrow Org_{(ads)} + xH_2O_{(sol)} \quad (7)$$

Where x: the number of water molecules replaced by one organic molecule. In this respect, the adsorption of the studied inhibitor was accompanied by desorption of water molecules from the carbon steel surface. In order to find the most suitable adsorption isotherm of inhibitor adsorption on carbon steel surface, data obtained from weight loss measurements has been used to fit different adsorption isotherms including: Langmuir, Temkin, and Frumkin isotherms. The best fit one was obtained with Langmuir's adsorption isotherm. This isotherm is given by the following equation [50]:

$$\frac{C_{inh}}{\theta} = \frac{1}{K_{ads}} + C_{inh} \quad (8)$$

where C_{inh} is the equilibrium inhibitor concentration, K_{ads} adsorptive equilibrium constant, θ representing the degree of adsorption (η_{WL}%/100).

The plot of C_{inh}/ θ vs. Cinh (Fig. 3) yields a straight line with correlation coefficient of 0.999 providing that the adsorption of Q1 from 1 M HCl solution on the carbon steel surface obeys Langmiur adsorption isotherm. The value of K_{ads} can be determined from the intercept of the straight line. K_{ads} is also related to the standard free energy of adsorption (ΔG°_{ads}) as [52]:

$$K_{ads} = \left(\frac{1}{55.5}\right)\exp\left(-\frac{\Delta G^{\circ}_{ads}}{RT}\right) \quad (9)$$

where R is gas constant and T is absolute temperature of experiment and the constant value of 55.5 is the concentration of water in solution in mol L^{-1}.

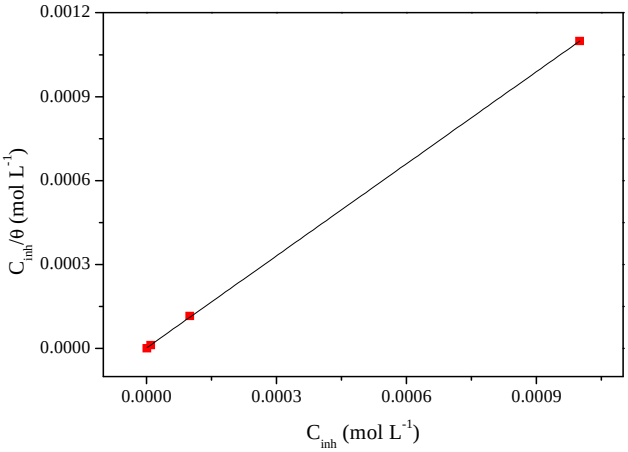

Figure 3: Langmuir adsorption of Q1on the carbon steel surface in 1 M HCl solution

The value of K_{ads} was found to be 383363.55 L mol^{-1}. The relatively high value of adsorption equilibrium constant reflects the high adsorption ability of Q1 on carbon steel surface [53]. It is well known that the values of ΔG°_{ads} of the order of -20 kJ mol^{-1} or lower indicate a physisorption; those of order of -40 kJ mol^{-1} or higher involve charge sharing or transfer from the inhibitor molecules to the metal surface to form a coordinate type of bond (chemisorption) [54-56]. On the other hand, the adsorption phenomenon of an organic molecule is not considered only as a purely physical or chemical adsorption phenomenon [57,58]. A wide spectrum of conditions, ranging from the dominance of chemisorption or electrostatic effects, arises from other adsorptions experimental data [59]. The value of -43.21 kJ mol^{-1} may suggest chemisorption mode.

Computational studies

To do research on the effect of geometric and electronic structural parameters on the inhibition efficiency of inhibitors, quantum chemical calculations were conducted. These studies are considered as powerful tools for studying their adsorption mechanisms about the metal surface [60]. In Figure 4, the improved molecular structures with minimum energies from the calculations are available.

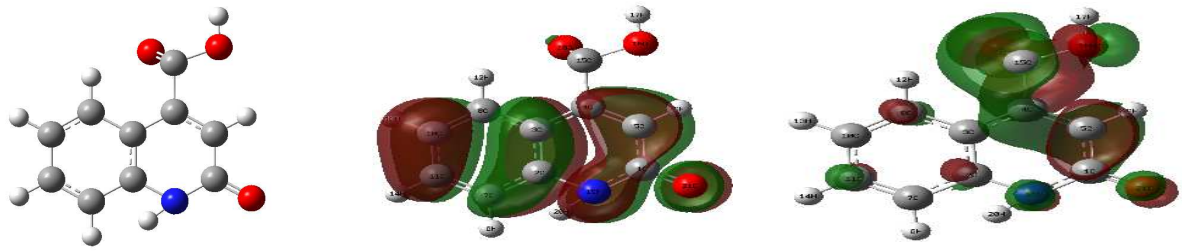

Figure 4: The optimized molecular structure, HOMO and LUMO (right) of the neutral inhibitor molecule by means of DFT/B3LYP/6-31G (d,p)

In Table 4, there are quantum chemical parameters from the calculations by means of DFT/B3LYP/6-31G (d,p) which are responsible for the inhibition efficiency of inhibitor, such as the energies of highest occupied molecular orbital (E_{HOMO}), energy of lowest unoccupied molecular orbital (E_{LUMO}), the separation energy (E_{LUMO}-E_{HOMO}), ΔE an ipole moment, μ, for the neutral inhibitor.

Table 4: calculated quantum chemical parameters for the neutral inhibitor

Paramters	E_{HOMO} (eV)	E_{LUMO} (eV)	ΔE (eV)	μ (D)
Q1	-9.2472	-1.8733	7.3739	4.6908

Recently, theoretical studies has been used to analyze the characteristics of the inhibitor/ surface mechanism and to describe the structural nature of the inhibitor in the corrosion process as well as analyze the experimental data. It has been found to be successful in providing insights into the chemical reactivity and selectivity in terms of global parameters the choosing of the quinoline derivative for use as a corrosion inhibitor due to contains oxygen and nitrogen atoms as active centers. It is well established in the literature that the higher the HOMO energy of the

inhibitor, the greater the trend of offering electrons to unoccupied d orbital of the metal, and the higher the corrosion inhibition efficiency. In addition, the lower the LUMO energy, as the LUMO-HOMO energy gap decreased and the efficiency of inhibitor improved. E_{HOMO} is often associated with the electron donating ability of a Q1. Therefore, increasing values of E_{HOMO} indicate a higher tendency for the donation of electron(s) to the appropriate acceptor molecule with low energy and an empty molecular orbital. Increasing values of E_{HOMO} thus facilitate the adsorption of the inhibitor. Consequently, improving the transport process through the adsorbed layer would enhance the inhibition efficiency of the inhibitor. This finding can be explained as follows. E_{LUMO} indicates the ability of the molecule to accept electrons; therefore, a lower value of E_{LUMO} more clearly indicates that the molecule would accept electrons [61].

The corresponding calculated quantum chemical data was given, including the energy of MOMO (E_{HOMO}=-9.2472 eV), energy of LUMO (E_{LUMO}=-1.8733 eV), the energy band gap (ΔE=7.3739 eV), and dipole moment (μ=4.6908 Debye). These results show that Q1 has a relatively higher energy of HOMO and lower energy of LUMO, which can be in favor of bonding with metal surface [62]. As a result of high values of HOMO, Q1 has a tendency to donate electrons to those acceptor molecules with empty molecular orbital. The ground-state electronic configuration of Fe atom is $1s^2\ 2s^2\ 2p^6\ 3s^2\ 3p^6\ 4s^2\ 3d^6$. The incompletely occupied 3P orbital of Fe could bond with HOMO of Q1, while the filled 3S orbital of it could interact with LUMO of Q1.

Furthermore, another important factor is worth noting that the influence of the dipole moment on corrosion inhibition was caused considerable concerns in a lot of literatures [63,64]. The dipole moment that is one of important electronic parameters arises from non-uniform distribution of charges on the various atoms in a molecule. The adsorption of Q1 can be regarded as a quasi-substitution process between the Q1 molecules and water molecules on the carbon steel surface [65].

CONCLUSION

The quinoline derivative was investigated as a new and effective corrosion inhibitor for carbonsteel in 1 M hydrochloric acid solution by a series of techniques. The following conclusions can be made from the experimental results:

- With an increase of the inhibitor concentration in acidic media inhibition is protected strongly.
- The quinoline derivative for carbon steel in 1 M HCl solution is a significant inhibitor and acts as the mixed type inhibitor.
- The adsorption behavior of Q1 on the carbon steel surface conforms to the Langmuir adsorption isotherm and the value of the free Gibbs energy of adsorption suggest a chemical adsorption.
- The quantum chemical calculations indicate that N and O atoms of Q1 molecule donate electrons to the incompletely occupied 3P orbital of Fe, and act as most probable nucleophilic centers to bond with metal iron surface.

REFERENCES

[1] M. Prajila, J. Sam, J. Bincy, J. Abraham, *J. Mater. Environ. Sci*. **2012**, 3, 1045.
[2] U.J. Naik, V.A. Panchal, A.S. Patel, N.K. Shah, *J. Mater. Environ. Sci*. **2012**, 3, 935.
[3] A. Zarrouk, H. Zarrok, R. Salghi, B. Hammouti, F. Bentiss, R. Touir, M. Bouachrine, J. *Mater. Environ. Sci*. **2013**, 4, 177.
[4] G. Avci, *Mater. Chem. Phys*. **2008**, 112, 234.
[5] A. Zarrouk, B. Hammouti, A. Dafali, F. Bentiss, *Ind. Eng. Chem. Res*. **2013**, 52, 2560.
[6] H. Zarrok, A. Zarrouk, R. Salghi, Y. Ramli, B. Hammouti, M. Assouag, E. M. Essassi, H. Oudda and M. Taleb, *J. Chem. Pharm. Res*., **2012**, 4, 5048.
[7] A. Ghazoui, R. Saddik, N. Benchat, M. Guenbour, B. Hammouti, S.S. Al-Deyab, A. Zarrouk, *Int. J. Electrochem. Sci*., **2012**, 7, 7080.
[8] H. Zarrok, S. S. Al-Deyab, A. Zarrouk, R. Salghi, B. Hammouti, H. Oudda, M. Bouachrine, F. Bentiss, *Int. J. Electrochem. Sci*. **2012**, 7, 4047.
[9] A. Zarrouk, B. Hammouti, H. Zarrok, M. Bouachrine, K.F. Khaled, S.S. Al-Deyab, *Int. J. Electrochem. Sci.*, **2012**, 6, 89.
[10] H. Zarrok, K. Al Mamari, A. Zarrouk, R. Salghi, B. Hammouti, S. S. Al-Deyab, E. M. Essassi, F. Bentiss, H. Oudda, *Int. J. Electrochem. Sci*., **2012**, 7, 10338.
[11] H. Zarrok, H. Oudda, A. El Midaoui, A. Zarrouk, B. Hammouti, M. Ebn Touhami, A. Attayibat, S. Radi, R. Touzani, *Res. Chem. Intermed*. **2012**, 38, 2051.
[12] A. Ghazoui, A. Zarrouk, N. Bencaht, R. Salghi, M. Assouag, M. El Hezzat, A. Guenbour, B. Hammouti, *J. Chem. Pharm. Res*. **2014**, 6, 704.

[13] H. Zarrok, A. Zarrouk, R. Salghi, H. Oudda, B. Hammouti, M. Assouag, M. Taleb, M. Ebn Touhami, M. Bouachrine, S. Boukhris, *J. Chem. Pharm. Res*. **2012**, 4, 5056.
[14] A. Zarrouk, H. Zarrok, R. Salghi, R. Touir, B. Hammouti, N. Benchat, L.L. Afrine, H. Hannache, M. El Hezzat, M. Bouachrine, *J. Chem. Pharm. Res*. **2013**, 5, 1482.
[15] H. Zarrok, A. Zarrouk, R. Salghi, M. Assouag, B. Hammouti, H. Oudda, S. Boukhris, S.S. Al Deyab, I. Warad, *Der Pharm. Lett*. **2013**, 5, 43.
[16] H. Zarrok, A. Zarrouk, R. Salghi, M. Ebn Touhami, H. Oudda, B. Hammouti, R. Touir, F. Bentiss, S.S. Al-Deyab, *Int. J. Electrochem. Sci*. **2013**, 8, 6014.
[17] D. Ben Hmamou, M.R. Aouad, R. Salghi, A. Zarrouk, M. Assouag, O. Benali, M. Messali , H. Zarrok, B. Hammouti, *J. Chem. Pharm. Res*. **2012**, 4, 3498.
[18] M. Belayachi, H. Serrar, H. Zarrok, A. El Assyry, A. Zarrouk, H. Oudda, S. Boukhris, B. Hammouti, Eno E. Ebenso, A. Geunbour, *Int. J. Electrochem. Sci*. **2015**, 10, 3010.
[19] H. Tayebi, H. Bourazmi, B. Himmi, A. El Assyry, Y. Ramli, A. Zarrouk, A. Geunbour, B. Hammouti, *Der Pharm. Chem*. **2014**, 6(5), 220.
[20] H. Tayebi, H. Bourazmi, B. Himmi, A. El Assyry, Y. Ramli, A. Zarrouk, A. Geunbour, B. Hammouti, Eno E.Ebenso, *Der Pharm. Lett*. **2014**, 6(6), 20.
[21] Y. ELaoufir, H. Bourazmi, H. Serrar, H. Zarrok, A. Zarrouk, B. Hammouti, A. Guenbour, S. Boukhriss, H. Oudda, *Der Pharm. Lett*. **2014**, 6(4), 526.
[22] H. Zarrok, A. Zarrouk, R. Salghi, H. Oudda, B. Hammouti, M. Ebn Touhami, M. Bouachrine, O.H. Pucci, *Port. Electrochim. Acta*, **2012**, 30, 405.
[23] Y. ELouadi, F. Abrigach, A. Bouyanzer, R. Touzani, O. Riant, B. ElMahi, A. El Assyry, S. Radi, A. Zarrouk, B. Hammouti, *Der Pharm. Chem*. **2015**, 7(8), 265.
[24] F. Benhiba, H. Zarrok, A. Elmidaoui, M, El Hezzat, R. Touir, A. Guenbour, A. Zarrouk, S. Boukhris, H. Oudda, *J. Mater. Environ. Sci*. **2015**, 6 (8), 2301.
[25] M. Belayachi, H. Zarrok, M. Larouj, A. Zarrouk, H. Bourazmi, A. Guenbour, B. Hammouti, S. Boukhriss, H. Oudda, *Phys. Chem. News* **2014**, 74, 85.
[26] L. Afrine, A. Zarrouk, H. Zarrok, R. Salghi, R. Touir, B. Hammouti, H. Oudda, M. Assouag, H. Hannache, M. El Harti, M. Bouachrine, *J. Chem. Pharm. Res*. **2013**, 5, 1474.
[27] A. Zarrouk, I. El Ouali, M. Bouachrine, B. Hammouti, Y. Ramli, E.M. Essassi, I. Warad, A. Aouniti, R. Salghi, *Res. Chem. Intermed*. **2013**, 39, 1125.
[28] A. Zarrouk, B. Hammouti, H. Zarrok, R. Salghi, M. Bouachrine, F. Bentiss, S. S. Al-Deyab, *Res. Chem. Intermed*. **2012**, 38, 2327.
[29] A. Zarrouk, B. Hammouti, H. Zarrok, S.S. Al-Deyab, I. Warad, *Res. Chem. Intermed*. **2012**, 38, 165.
[30] M. El Hezzat, M. Assouag, H. Zarrok, Z. Benzekri, A. El Assyry, S. Boukhris, A. Souizi, M. Galai, R. Touir, M. Ebn Touhami, H. Oudda, A. Zarrouk, *Der Pharm. Chem*. **2015**, 7(10), 77
[31] S. EL Arouji, K. Alaoui Ismaili, A. Zerrouki, S. El Kadiri, Z. Rais, M. Filali Baba, M. Taleb, Khadijah M. Emran, A. Zarrouk, A. Aouniti, B. Hammouti, *Der Pharm. Chem*. **2015**, 7(10), 67.
[32] K.C. Emregüül, M. Hayvalı, *Mater. Chem. Phys*. **2004**, 83, 209.
[33] M.K. Awad, M.R. Mustafa, M.M.A. Elnga, *J. Mol. Struct. (THEOCHEM)* **2010**, 959, 66.
[34] B.D. Mert, M.E. Mert, G. Kardaş, B. Yazıcı, *Corros. Sci*. **2011**, 53, 4265.
[35] Arumugam Manivel, Sekar Ramkumar, Jerry J. Wu, Abdullah M. Asiri, Sambandam Anandan, *J. Environ. Chem. Eng*. **2014**, 2, 463.
[36] Ime B. Obot, Eno E. Ebenso, Mwadham M. Kabanda, *J. Environ. Chem. Eng*. **2013**, 1, 431.
[37] A.Y. Musa, R.T.T. Jalgham, A.B. Mohamad, Corros. Sci. **2012**, 56, 176.
[38] ASTM, G 31-72, American Society for Testing and Materials, Philadelphia, PA, **1990**.
[39] A. D. Becke, *J. Chem. Phy*. **1992**, 96, 9489.
[40] A. D. Becke, *J. Chem. Phy*. **1993**, 98, 1372.
[41] C. Lee, W. Yang, R.G. Parr, *Phy. Rev. B* **1988**, 37, 785.
[42] M.J. Frisch, G.W. Trucks, H.B. Schlegel, G.E. Scuseria, M.A. Robb, J.R. Cheeseman, J.A. Montgomery Jr., T. Vreven, K.N. Kudin, J.C. Burant, J.M. Millam, S.S. Iyengar, J. Tomasi, V. Barone, B. Mennucci, M. Cossi, G. Scalmani, N. Rega, G.A. Petersson, H. Nakatsuji, M. Hada, M. Ehara, K. Toyota, R. Fukuda, J. Hasegawa, M. Ishida, T. Nakajima, Y. Honda, O. Kitao, H. Nakai, M. Klene, X. Li, J.E. Knox, H.P. Hratchian, J.B. Cross, C. Adamo, J. Jaramillo, R. Gomperts, R.E. Stratmann, O. Yazyev, A.J. Austin, R. Cammi, C. 870 H. Ju et al. / Corrosion Science 50 (2008) 865-871 Pomelli, J.W. Ochterski, P.Y. Ayala, K. Morokuma, G.A. Voth, P. Salvador, J.J. Dannenberg, V.G. Zakrzewski, S. Dapprich, A.D. Daniels, M.C. Strain, O. Farkas, D.K. Malick, A.D. Rabuck, K. Raghavachari, J.B. Foresman, J.V. Ortiz, Q. Cui, A.G. Baboul, S. Clifford, J. Cioslowski, B.B. Stefanov, G. Liu, A. Liashenko, P. Piskorz, I. Komaromi, R.L. Martin, D.J. Fox, T. Keith, M.A. Al- Laham, C.Y. Peng, A. Nanayakkara, M. Challacombe, P.M.W. Gill, B. Johnson, W. Chen, M.W. Wong, C. Gonzalez, J.A. Pople, Gaussian 03, Revision C.02, Gaussian Inc., Pittsburgh, PA, **2003**.
[43] E. Barmatov, T. Hughes, M. Nagl, *Corros. Sci*. **2014**, 81, 162.

[44] K.F. Khaled, M.A. Amin, *Corros. Sci*. **2009**, 51, 1964.
[45] A. Anejjar, R. Salghi, A. Zarrouk, O. Benali, H. Zarrok, B. Hammouti, E.E. Ebenso, J. *Asso. Arab. Univ. Basic. App. Sci*. **2014**, 15, 21.
[46] K. Zakarya, A.A. Farag, W. Ahmed, I.M. Nassar, *Int. J. Adv. Sci.Technol. Res*. **2014**, 4, 196.
[47] A.A. Farag, W. Ahmed, K. Zakaria, I.M. Nassar, *Int. J. Sci. Res*. **2014**, 3, 870.
[48] N.A. Negm, A.M. ElSabagh, M.A. Migahed, H.M. AbdelBary, H.M. ElDin, *Corros. Sci*. **2010**, 52, 2122.
[49] N.A. Negm, N.G. Kandile, M.A. Mohammed, E.A. Bedr, *Corros. Sci*. **2012**, 65, 94.
[50] N.A. Negm, F.M. Ghuiba, S.M. Tawfik, *Corros. Sci*. **2011**, 53, 3566.
[51] L. Li, Q. Qu, W. Bai, F.C. Yang, Y.J. Chen, S.W. Zhang, Z.T. Ding, *Corros. Sci*. **2012**, 59, 249.
[52] M.J. Bahrami, S.M.A. Hosseini, P. Pilvar, *Corros. Sci*. **2010**, 52, 2793.
[53] M.A. Migahed, *Mater. Chem. Phys*. **2005**, 93, 48.
[54] I. Ahamad, R. Prasad, M.A. Quraishi, *Corros. Sci*. **2010**, 52, 933.
[55] E.A. Noor, A.H. Al-Moubaraki, *Mater. Chem. Phys*. **2008**, 110, 145.
[56] M. Özcan, R. Solmaz, G. Kardas, I. Dehri, *Colloids Surf. A* **2008**, 325, 57.
[57] R. Solmaz, *Corros. Sci*. **2010**, 52, 3321.
[58] A. Döner, R. Solmaz, M. Özcan, G. Kardas, *Corros. Sci*. **2011**, 53, 2902.
[59] G. Moretti, F. Guidi, G. Grion, *Corros. Sci*. **2004**, 46, 387.
[60] M. J. S. Dewar, E. G. Zoebisch, E. F. Healy, and J. J. P. Stewart, *J. Am. Chem. Soc*. **1985**, 107, 3902.
[61] J.M. Costa, J.M. Lluch, *Corros. Sci*. **1984**, 24, 924.
[62] G. Bereket, C. Ogretir and C.Ozsahim, *J. Mol. Struct. (THEOCHEM)*. **2003**, 663, 39.
[63] G. Gece, *Corros. Sci*. **2008**, 50, 2981.
[64] N. Khalil, *Electrochim. Acta*. **2003**, 48, 2635.
[65] W. Chen, S. Hong, H. B. Li, H. Q. Luo, M. Li and N. B. Li, *Corros. Sci*. **2012**, 61, 53.